SCIENTIFIC REPORT ON THE EXCHANGE TRAVEL GRANT OF THE ESF NETWORK "NEWFOCUS" DECEMBER, 2011 – FEBRUARY, 2012 VISIT FROM IRE NASU, KHARKIV, UKRAINE TO GGIEMR, THE UNIVERSITY OF NOTTINGHAM, NOTTINGHAM, UNITED KINGDOM

TOPIC: "INVESTIGATION OF 3-D ROTATIONALLY SYMMETRIC METAL AND DIELECTRIC RESONATORS"

Purpose of the visit is high-accuracy modeling of 3-D axially symmetric dielectric and metal resonators. Microwave resonators are used in a variety of application, including filters, oscillators, frequency meters and tuned amplifiers. Dielectric resonators are smaller in cost, size and weight than an equivalent metallic cavity. However, accurate mathematical modeling of dielectric resonators is harder then modeling of metallic cavity because the first is the whole space problem and the second is the problem for finite part of space inside the cavity.
We use Muller integral equations (IEs) to model the dielectric resonators. They are 2-D Fredholm second kind IEs with equivalent magnetic and electric currents as unknowns. For axially symmetric bodies we represent currents as Fourier series and reduce 2-D Muller IEs to the set of 1-D IE system for each azimuthal order. Each of these systems has four unknown functions: two components of electric equivalent current and two components of magnetic equivalent current. To descritize these systems we interpolate each term of the current-function Fourier series by Legendre polynomials and use quadrature formulas of interpolation type.
Firstly, we compare results of numerical experiment with analytical solution for a sphere. Then we investigate Q-factors and eigenfields for spheroids in the case of modes with zero azimuthal order. The purpose of this study is finding an oblate or prolate spheroid with a higher quality factor than the dielectric sphere quality factor.
Secondly, we consider finite dielectric circular cylinder and calculate resonance frequencies, Q-factors, and eigenfields, and compare these data with real experiments and other theoretical methods.

Description of the work carried out during the visit

Suppose that $\left(\vec{E}_m, \vec{H}_m\right)$ is the total field inside the region V_m, $m = 1, 2$. It can be represented in the form of the sum of the incident and scattered ones $\left(\vec{E}_m, \vec{H}_m\right) = \left(\vec{E}_m^{inc}, \vec{H}_m^{inc}\right) + \left(\vec{E}_m^{s}, \vec{H}_m^{s}\right)$. Boundary conditions require that the total field tangential to the surface of the body is continuous from region V_1 to region V_2 (Fig.1).

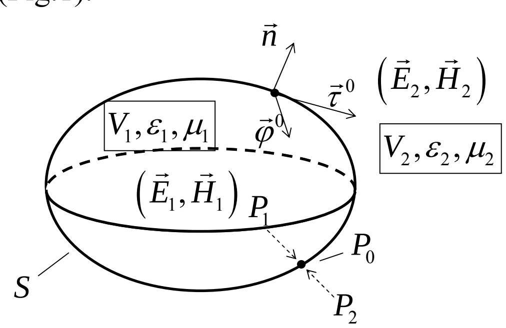

Fig. 1. Dielectric body of revolution and notations

These conditions can be expressed as

$$\lim_{P_2\to P_0}\left[\vec{E}_2(P_2),\vec{n}\right]=\lim_{P_1\to P_0}\left[\vec{E}_1(P_1),\vec{n}\right],\ \lim_{P_2\to P_0}\left[\vec{H}_2(P_2),\vec{n}\right]=\lim_{P_1\to P_0}\left[\vec{H}_1(P_1),\vec{n}\right], \tag{1}$$

where vector $\vec{n}$ is a unit normal vector to the surface S directed outside (to the region V_2), ε_m,μ_m are dielectric and magnetic permittivities, respectively , $\vec{\tau}^0,\vec{\varphi}^0$ are tangential vectors to rotation surface S .
Scattered electric and magnetic fields are expressed through equivalent magnetic and electric current densities $\vec{j}^e_m(P_0)=\left[\vec{n}_m,\vec{H}_m(P_0)\right]$, $m=1,2$, $\vec{j}^e_m(P_0)=\left[\vec{n}_m,\vec{H}_m(P_0)\right]$, $m=1,2$ as follows:

$$\begin{pmatrix}\vec{E}^s_p\\ \vec{H}^s_p\end{pmatrix}=\begin{pmatrix}\vec{E}^{inc}_p\\ \vec{H}^{inc}_p\end{pmatrix}-\iint_S\begin{pmatrix}\frac{i}{\varpi\varepsilon_p}\left(\nabla\nabla+k^2\right)G_p & \nabla\times G_p\\ -\nabla\times G_p & \frac{i}{\varpi\mu_p}\left(\nabla\nabla+k^2\right)G_p\end{pmatrix}\begin{pmatrix}\vec{j}^e_p\\ \vec{j}^m_p\end{pmatrix}dS,\ p=1,2, \tag{2}$$

where $G_m=\frac{1}{4\pi}\frac{\exp(ik_mR)}{R},m=1,2$ is the Green's function of the free space of parameters of the region V_m , $m=1,2$, $\vec{n}_m$ is the normal, directed to region V_m , $m=1,2$.
Using (1) and (2) one can obtain the Muller integral equations (IEs),

$$\begin{pmatrix}-\vec{j}^m(P_0)\frac{\varepsilon_2+\varepsilon_1}{2}\\ \vec{j}^e(P_0)\frac{\mu_2+\mu_1}{2}\end{pmatrix}=\vec{n}\times\begin{pmatrix}\varepsilon_2\vec{E}^{inc}_2(P_0)+\varepsilon_1\vec{E}^{inc}_1(P_0)\\ \mu_2\vec{H}^{inc}_2(P_0)+\mu_1\vec{H}^{inc}_1(P_0)\end{pmatrix}-$$
$$-\vec{n}\times\iint_S\begin{pmatrix}\frac{i}{\varpi}\left[\nabla\nabla(G_2-G_1)+k_2^2G_2-k_1^2G_1\right] & \nabla\times(\varepsilon_2G_2-\varepsilon_1G_1)\\ -\nabla\times(\mu_2G_2-\mu_1G_1) & \frac{i}{\varpi}\left[\nabla\nabla(G_2-G_1)+k_2^2G_2-k_1^2G_1\right]\end{pmatrix}\begin{pmatrix}\vec{j}^e\\ \vec{j}^m\end{pmatrix}dS, \tag{3}$$

where $-\vec{j}^m_1=\vec{j}^m_2=\vec{j}^m$, $-\vec{j}^e_1=\vec{j}^e_2=\vec{j}^e$.

For the body of revolution electric and magnetic current densities are represented as Fourier series in azimuth,

$$\vec{j}_\nu(t,\varphi)=\sum_{M=-\infty}^{\infty}\vec{j}_\nu^{(M)}(t)e^{iM\varphi},\ \nu=\tau,\varphi \tag{4}$$

Substituting (3) to (2), we obtain that for axially-symmetric bodies 2-D Muller IEs reduce to a set of 1-D IEs. In the kernels of these IEs, we separate the logarithmic singularities. As a result, we obtain the system of 4 IEs for each azimuthal harmonic of electric and magnetic currents,

$$J^{(M)}(\tau)+\int_{-1}^{1}A^{(M)}(\tau)J^{(M)}(t)\ln|\tau-t|dt+\int_{-1}^{1}K^{(M)}(\tau,t)J^{(M)}(t)dt=F^{(M)}(\tau), \tag{5}$$

where $J^{(M)}=\left(J^{e(M)}_\tau,J^{e(M)}_\varphi,J^{m(M)}_\tau,J^{m(M)}_\varphi\right)$,

$$F_1^{(M)} = \frac{\mu_1}{\mu_1+\mu_2}\vec{H}_{1\varphi}^{(M)inc} + \frac{\mu_2}{\mu_1+\mu_2}\vec{H}_{2\varphi}^{(M)inc},\ F_2^{(M)} = \frac{\mu_1}{\mu_1+\mu_2}\vec{H}_{1\tau}^{(M)inc} + \frac{\mu_2}{\mu_1+\mu_2}\vec{H}_{2\tau}^{(M)inc},$$
$$F_3^{(M)} = \frac{\mu_1}{\mu_1+\mu_2}\vec{E}_{1\varphi}^{(M)inc} + \frac{\mu_2}{\mu_1+\mu_2}\vec{E}_{2\varphi}^{(M)inc}, F_4^{(M)} = \frac{\varepsilon_1}{\varepsilon_1+\varepsilon_2}\vec{E}_{1\varphi}^{(M)inc} + \frac{\varepsilon_2}{\varepsilon_1+\varepsilon_2}\vec{E}_{2\varphi}^{(M)inc}$$

$A^{(M)}(\tau)$ and $K^{(M)}(\tau,t)$ are the matrices 4×4, with elements $A_{l,m}^{(M)}(\tau)$ и $K_{l,m}^{(M)}(\tau,t)$ $l,m=1,2,3,4$ respectively. The elements $A_{l,m}^{(M)}(\tau)$ are infinitely differentiable functions and $K_{l,m}^{(M)}(\tau,t)\in C_{[-1,1]\times[-1,1]}^{2-\delta}$, where $\delta>0$.

To discretize IEs (5), we use quadrature formulas of interpolation type for the integrals with logarithmic and smooth kernels. The interpolation points are Legendre polynomial zeros. Using these quadrature formulas, we obtain the system of linear algebraic equation (SLAE) for interpolation points of currents interpolation polynomials,

$$A^{(M)}y^{(M)} = b^{(M)}, \tag{6}$$

where $y^{(M)}$ is approximate values of the M-th azimuthal harmonic of electric and magnetic currents in the Legendre polynomial zeros, vector $b^{(M)}$ is expressed through the values of primary field $F^{(M)}$ M-th azimuthal harmonic in Legendre polynomial zeros. Eigenfields are the fields, which can exist without primary field. They are expressed through equivalent currents, using (2), in the case of $\vec{E}_p^{inc} = \vec{H}_p^{inc} = 0, p=1,2$

Electric and magnetic eigencurrents are solutions of (5) in the case of $F^{(M)}(\tau)=0$. The corresponding approximate discrete equation is (6) in the case of $b^{(M)}=0$. The matrix $A^{(M)}$ depends on the wavenumber. Approximate values of the resonance wavenumber are such ones for which SLAE (6) has a nonzero solution for the zero right side, i.e. they are solutions of the following equation:

$$\left|A^{(M)}(k)\right| = 0, \tag{7}$$

where $\left|A^{(M)}(k)\right|$ is the determinant of the matrix $A^{(M)}$ as a function of the wavenumber. To find a solution of (7), one can consider, for example, function $f(k_1,k_2)=\left|A^{(M)}(k_1+ik_2)\right|$ and find its minima using the gradient method. However, holomorphicity of the complex-valued function of complex argument $\left|A^{(M)}(k)\right|$ allows constructing more efficient method to find eigenvalue wavenumbers. For that we approximate $\left|A^{(M)}(k)\right|$ using a complex-valued interpolation polynomial with complex coefficients and then find its zeros using Laguerre method. Further the solution of (6) with a zero right-hand side is determined using Gaussian elimination method for the obtained eigenvalue wavenumber. This solution is a vector of eigencurrent approximate values in Legendre polynomial zeros. Through these values, eigenfields are expressed using the expression (2) and interpolation type quadrature formulas.

Firstly, we can compare the results of described algorithm with analytical solutions for a dielectric sphere. The eigenfrequencies of dielectric sphere are the roots α of the following equations [1]:

$$TM: \quad \frac{J_{n-1/2}(m\alpha)}{J_{n+1/2}(m\alpha)} = m\frac{H^{(2)}_{n-1/2}(m\alpha)}{H^{(2)}_{n+1/2}(m\alpha)} - \frac{n}{\alpha}\frac{m^2-1}{m}, \tag{8}$$

$$TE: \quad \frac{J_{n-1/2}(m\alpha)}{J_{n+1/2}(m\alpha)} = \frac{1}{m}\frac{H^{(2)}_{n-1/2}(m\alpha)}{H^{(2)}_{n+1/2}(m\alpha)}, \tag{9}$$

$m=\sqrt{\varepsilon}$, ε is dielectric permittivity.

For example, using (8) and (9) we obtain the following eigenfrequencies in the case $\varepsilon = 10$ (in any other case we will consider only this dielectric permittivity): $(ka)_{res} = 1.685800 + 0.055470i$ for the mode TM^r_{021}, $(ka)_{res} = 1.775602 + 0.007603i$ for the mode TE^r_{031}. In Figs. 2, 3, we show relative error of presented method in the case of these modes

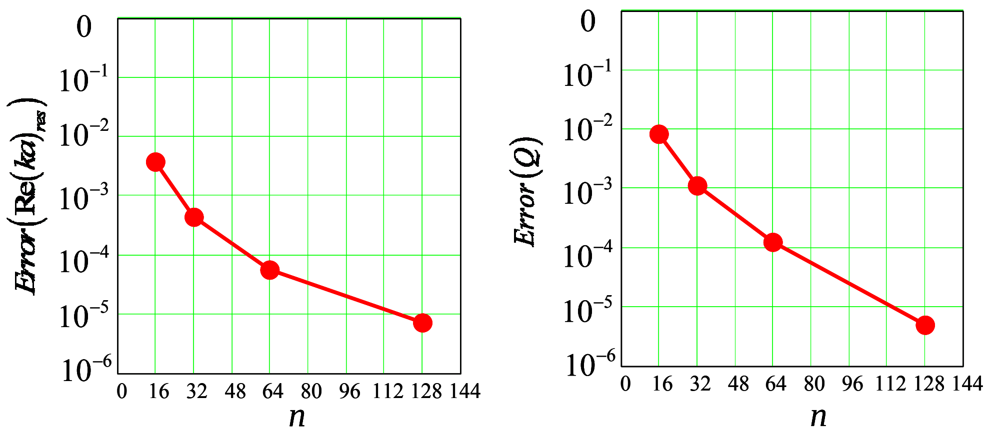

Fig.2 Relative error of the real part (left) of the eigenfrequency (right) and the quality-factor for the TM^r_{021} mode.

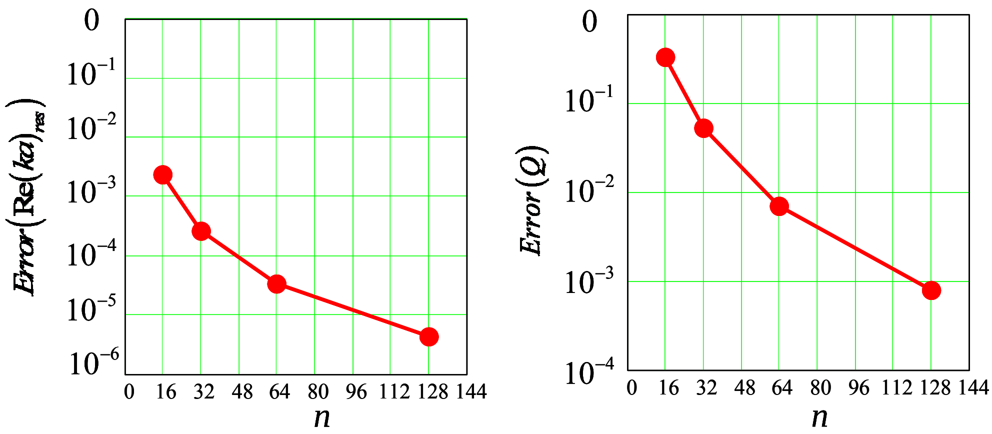

Fig.3 Relative error of the real part of the eigenfrequency (left) and the quality-factor (right) for the TE^r_{031} mode.

The eigenfields of the TM^r_{041} and TM^r_{051} modes are shown in Fig.4. Corresponding values of the eigenfrequencies are 2.502083+i0.003448 and 2.885163+i0.000834.

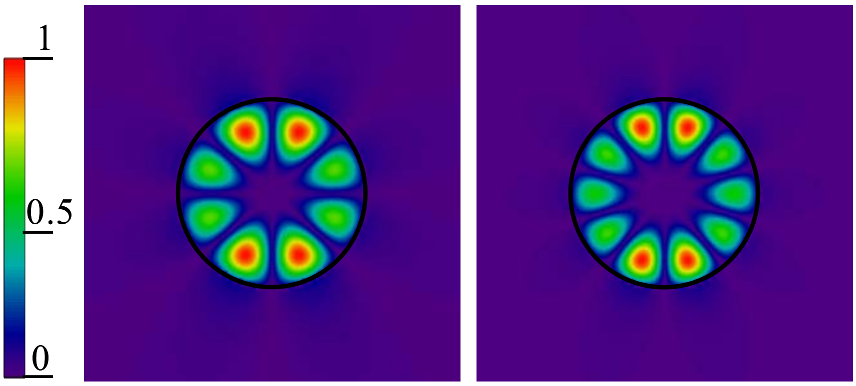

Fig.4. The TM^{r}_{041} and TM^{r}_{051} mode eigenfields in the dielectric sphere with $\varepsilon = 10$

In addition, the diffraction problem has been also solved. Suppose that a dielectric sphere is excited by an elementary dielectric dipole located inside the sphere as shown in Fig.5 (left) with the wavenumber, which equals to the real part of the TM^{r}_{041} mode eigenwavenumber. We obtain a field very similar to the TM^{r}_{041} field (Fig.5, right).

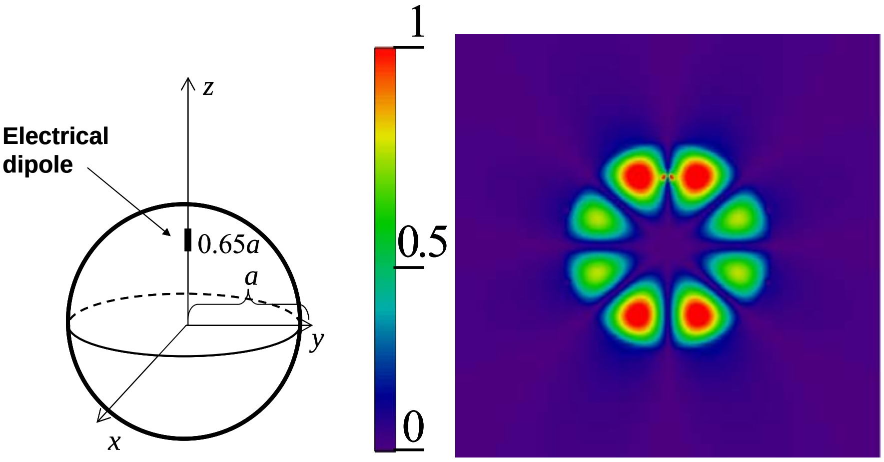

Fig.5. Dielectric sphere $\varepsilon = 10$ excited by dielectric dipole with ka=2.502083

As a demonstration of the diffraction program I show in Fig 6,7 fields of dielectric sphere illuminated by the electrical dipole placed inside and outside the sphere.

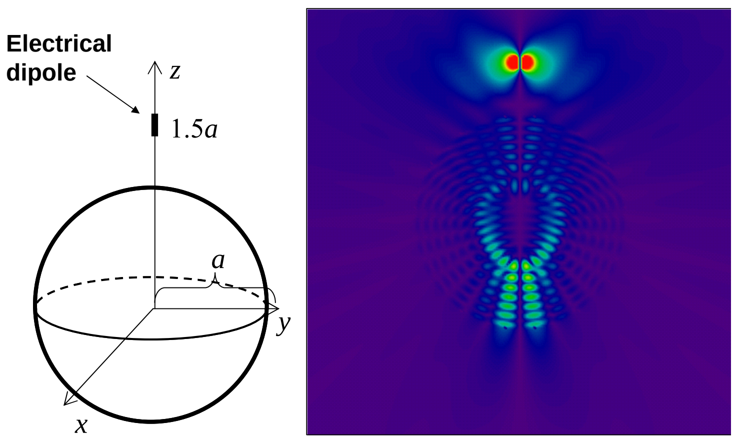

Fig.6. Dielectric sphere with ka=4π and $\varepsilon = 10$ excited by a dielectric dipole placed outside the sphere.

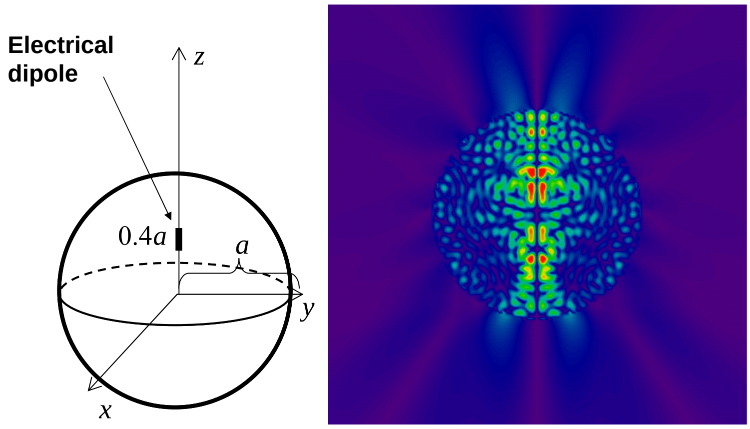

Fig.7. Dielectric sphere with ka=4π and $\varepsilon = 10$ excited by a dielectric dipole placed inside the sphere.

Spherical dielectric resonators are widely used in microwave engineering. Characteristic equations for dielectric sphere eigenfrequencies and eigenfields are well known. An interesting question can be formulated: can we deform a dielectric sphere so that the same mode in the obtained dielectric prolate or oblate spheroid would have larger quality factor than the dielectric sphere? The answer to this question is given in Fig.8, where quality-factor $Q = \frac{\mathrm{Re}(k_{res})}{2 \cdot \mathrm{Im}(k_{res})}$ as a function of spheroid deformation parameter b/a is shown for the mode TM_{011}. In Fig.8, we see that spheroids having $b/a = 0.4$ and $b/a = 2.9$ give almost twice larger Q-factors than the dielectric spherical resonator corresponding to $b/a = 1$. In Fig. 9, we show magnetic eigenfields for three cases $b/a = 0.4,\ 1,\ 2.9$ for the considered mode.

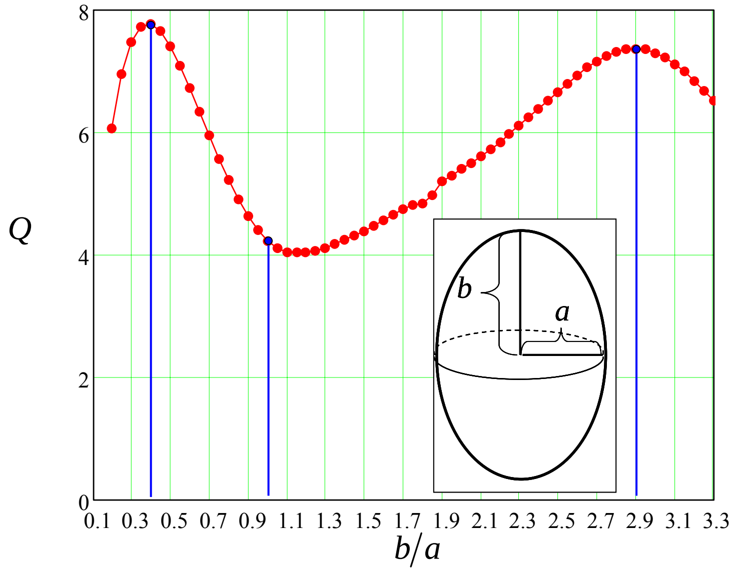

Fig. 8. Quality factor as a function of spheroid deformation parameter b/a for the TM_{011} mode, $\varepsilon = 10$.

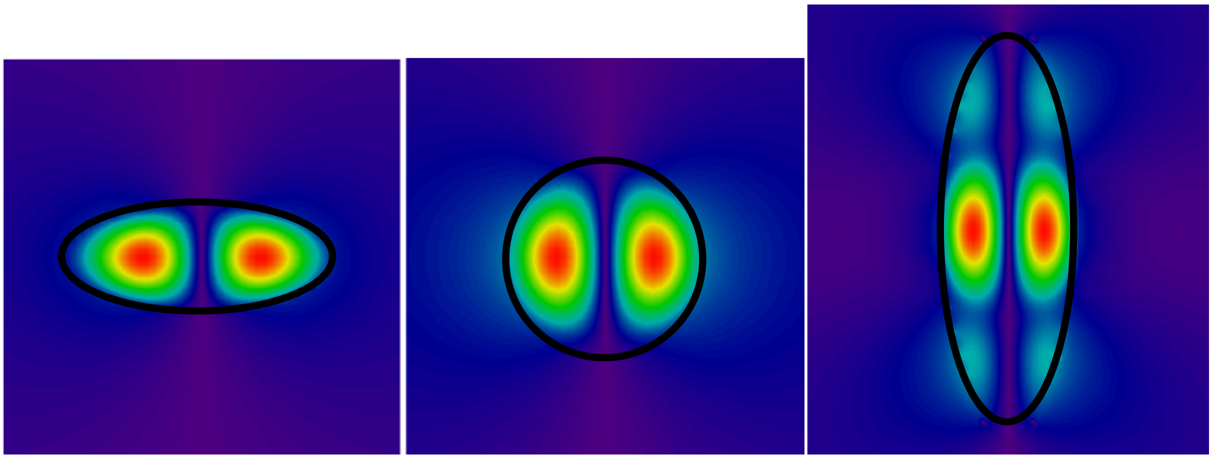

Fig.9. Magnetic eigenfield for spheroids $b/a = 0.4,\ 1,\ 2.9$ in the case of TM_{011} mode

\

Dielectric spheroid with $b/a = 0.85$ has slightly larger Q-factor than the dielectric sphere in the case of the TM_{021} mode as shown in Fig.10.

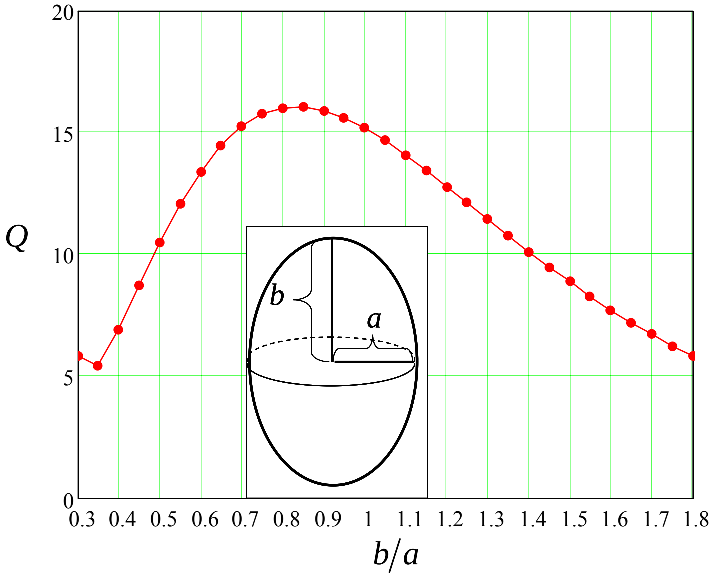

Fig. 10. Quality factor as a function of spheroid deformation parameter b/a for the TM_{021} mode, $\varepsilon = 10$

Numerical experiment shows that for the higher orders modes spherical resonator gives the best Q-factor (for zero azimuth index). As an example we show in Fig.11 the Q-factor as a function of spheroid deformation parameter b/a for the mode TE_{031}.

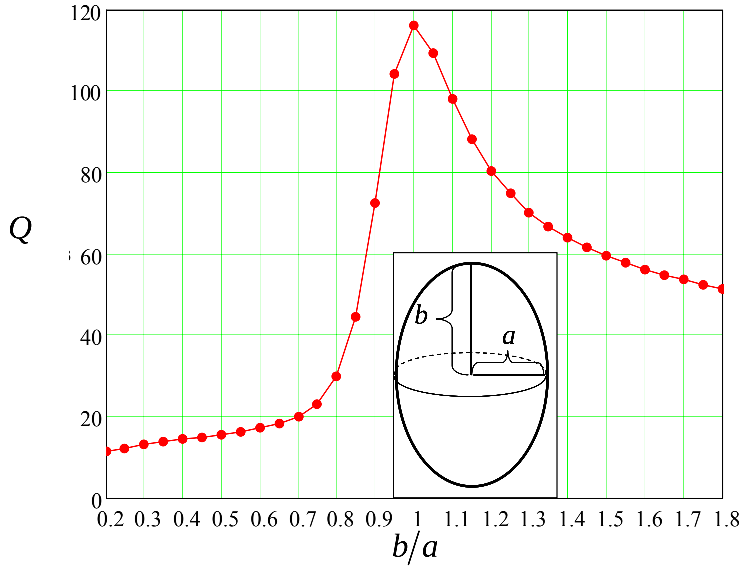

Fig. 11. Quality factor as a function of spheroid deformation parameter b/a for the TE_{031} mode, $\varepsilon = 10$

Now consider a cylindrical dielectric resonator created by rotation of rectangular contour. We approximate this rectangle by a super-ellipse as shown in Fig.12.

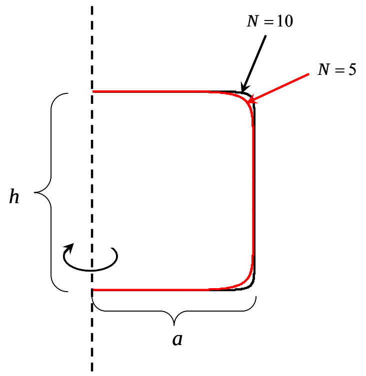

Fig.12 A half of super-ellipse of the order $N = 5,10$

Compare results of our numerical experiments with real experiments from [2,3]. Table 1 and Table 2 present the data for a dielectric pillbox with a = 5.25 mm, h = 4.6 mm, $\varepsilon = 38$. In Table 3 presented are the data for dielectric pillboxes of (1) diameter=12.83, height=5.62, $\varepsilon = 38$ and (2) diameter = 10.29 mm, height = 4.51mm, $\varepsilon = 79.7$

	Computed by our method	Measured [1]	Measured [2]
$TE_{01\delta}$	0.534	0.533	0.533
$TM_{01\delta}$	0.829	0.824	0.836

Table 1 Comparison of experimental and computed by our method normalized resonant wavelengths for a dielectric pillbox a = 5.25 mm, h = 4.6 mm, $\varepsilon = 38$ (height/diameter=0.4381)

	Computed by our method	Measured [1]	Measured [2]
$TE_{01\delta}$	40.89	51	46.4
$TM_{01\delta}$	78.66	86	58.1

Table 2. Comparison of experimental and computed by our method quality factors for a dielectric pillbox with *a* = 5.25 mm, *h* = 4.6 mm, $\varepsilon = 38$ (height/diameter=0.4381)

	Computed frequency(GHz)	Measured frequency(GHz)	Computed Q-factor	Measured Q-factor
1) $TE_{01\delta}$	3.984	3.967	40.9	46.4
1) $TM_{01\delta}$	6.169	6.133	77.8	58.1
2) $TE_{01\delta}$	3.474	3.479	111.3	118.9
2) $TM_{01\delta}$	5.392	5.407	466.5	416.9

Table 3. Comparison of experimental and computed by our method resonance frequencies and quality factors for dielectric pillboxes of (1) diameter=12.83, height=5.62, $\varepsilon = 38$ and (2) diameter = 10.29 mm, height = 4.51mm, $\varepsilon = 79.7$

We compare the results of presented method with the results of other theoretical methods for a dielectric circular cylinder [4-6] and show them in Tables 4 and 5.

	Our method	Theory [3]	Theory [4]	Theory [5]
$TE_{01\delta}$	0.534	0.531	0.534	0.53
$TM_{01\delta}$	0.829	0.827	0.829	0.827

Table 4. Comparison of normalized resonant wavelength computed by our method with ones computed by the methods [4-6] for dielectric pillbox for dielectric pillbox a = 5.25mm, h = 4.6mm, $\varepsilon = 38$.

	Our method	Theory [3]	Theory [4]	Theory [5]
$TE_{01\delta}$	40.89	45.8	40.8	47
$TM_{01\delta}$	78.66	86	76.9	71

Table 5. Comparison of quality factors computed by our method with ones computed by the methods [4-6] for a dielectric pillbox with *a* = 5.25 mm, *h* = 4.6 mm, $\varepsilon = 38$.

In Fig.13, the lowest modes of a dielectric circular resonator in the logarithmic scale are shown. They are in good agreement with data of [4]

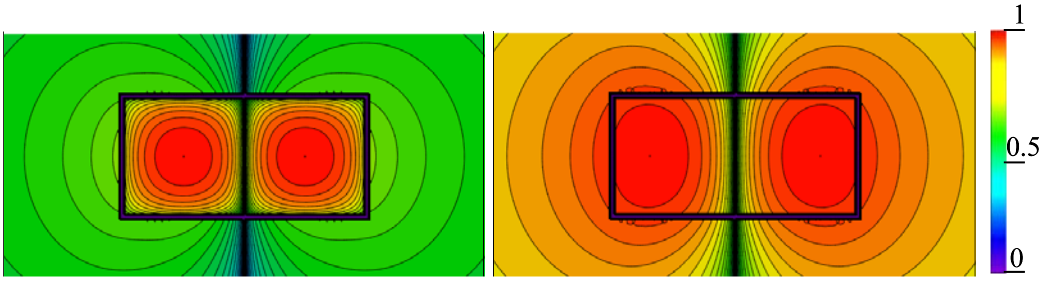

Fig.13. Magnetic field patterns for the $TM_{01\delta}$ and $TE_{01\delta}$ modes of a dielectric circular cylindrical resonator with $a = 5.25$mm, $h = 4.6$mm, $\varepsilon = 38$.

References

[1] P. Affolter and B Eliasson, "Electromagnetic resonances and Q-Factors of lossy dielectric spheres," *IEEE Trans. Microwave Theory and Techniques*, vol. MTT-21, no 9, 1973

[2] A. W. Glisson, D. Kajfez, and J. James, "Evaluation of modes in dielectric resonators using a surface integral equation formulation," *IEEE Trans. Microwave Theoiy Tech.*, vol. MTT-31, pp. 1023-1029, Dec. 1983.

[3] R. K. Mongia, C. L. Larose, S. R. Mishra and P. Bhartia "Accurate measurement of Q-Factors of isolated dielectric resonators "*IEEE Trans. Microwave Theory and Techniques,* vol.42 no.8, pp. 1463-1467, Dec. 1994.

[4] D. Kajfez, A. W. Glisson and J. James, "Computed modal field distribution for isolated dielectric resonators," *IEEE Trans. Microwave Theory and Techniques*, vol. MTT-32, pp. 1609-1616, 1984.

[5] W. Zheng, "Computation of complex resonance frequencies of isolated composite objects," *IEEE Trans. Microwave Theory and Techniques*, vol. 37, pp. 953-961, June 1989.

[6] J. A. Pereda, L.A. Vielva, A. Vegas, and A. Prieto, "Computation of resonant frequencies and quality factors of open dielectric resonators by a combination of the finite-difference time-domain (FDTD) and Prony's methods," *IEEE Microwave and Guided Wave Lett*ers, vol. 2, pp. 431-433, Nov. 1992.

Publications based on the project work (in work or submitted):

Conference paper

V.S. Bulygin, A. Vukovic, T.M. Benson, P.Sewell, A.I. Nosich, "3D modelling of thin disc resonators", *ICTON-2012,* Coventry.

Journal paper

V. S. Bulygin, Y. V. Gandel, A. I. Nosich, T. M. Benson, "Full-wave analysis and optimization of a TARA-like shielded-assisted paraboloidal reflector antenna using Nystrom-type method," *IEEE Trans. Antennas and Propagation* (in preparation).